THE JOURNAL OF PHYSICAL CHEMISTRY B

Article

pubs.acs.org/JPCB

A Direct SAXS Approach for the Determination of Specific Surface Area of Clay in Polymer-Layered Silicate Nanocomposites

Carla Marega, Valerio Causin,* Roberta Saini, and Antonio Marigo

Dipartimento di Scienze Chimiche, Università di Padova, via Marzolo 1, 35131 Padova, Italy

A. P. Meera and Sabu Thomas

School of Chemical Sciences, Mahatma Gandhi University, Kottayam, Kerala, India 686560

K. S. Usha Devi

Department of Chemistry, NSS College, Pandalam, Kerala, India 689501

ABSTRACT: The interfacial area between the matrix and the filler is a key parameter which shapes the performance of polymer-based composites and nanocomposites, even though it is difficult to quantify. A very easy SAXS method, based on the Porod equation, is proposed for measuring the specific surface area of nanofillers embedded in a polymer matrix. In order to assess its reliability, this approach was applied to natural rubber- or styrene butadiene-based samples containing different types of montmorillonite clay. A wide range of specific surfaces was detected. SAXS data were compared to complementary X-ray diffraction and TEM information, obtaining a good agreement. Interpretation of the tensile properties by theoretical models and comparison with the literature corroborated the validity of the specific surface area measurement. The possibility to quantify this feature of composites allows the rational design of such materials to be improved.

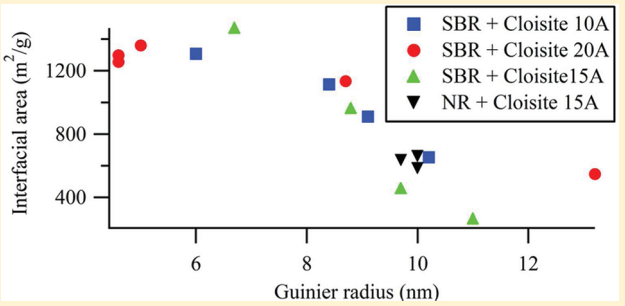

1. INTRODUCTION

A large amount of research work has been done on polymer−clay nanocomposites since the pioneering intuition of the Toyota group.[1] Although remarkable results have been achieved,[2,3] the improvement of physical mechanical properties did not fully reach the expectations.[4] The basic insight that brought to the development of the nanocomposite approach is that, if the size of fillers used in polymer composites were decreased to the nanometer range, then a dramatic increase in contact surface could be attained. If this large interfacial area is coupled with strong interaction, a considerable increase in strength and stiffness is expected with very low filler content.[5,6]

The physical mechanical properties of all heterogeneous polymer systems including nanocomposites are determined by four main factors:[7] component properties, composition, structure, and interfacial interactions. The most important filler characteristics are particle size, shape, size distribution, and specific surface area. Structure is determined by segregation, aggregation, and/or orientation phenomena. Interfacial interactions, which can be tuned by surface modification, shape the properties of the interphase, and thus the macroscopic performance. Among the cited factors, established TEM,[8] WAXD, and SAXS[9−14] techniques allow for the investigation and quantification of the size and morphology of dispersion of the filler in the matrix. As an example of the potential of SAXS analyses, for example, Krishnamoorti and colleagues exploited the anisotropy factor evaluated by SAXS to investigate shear induced orientation phenomena in polymer/clay dispersions[15] or highlighted the disruptive effects that clay has on polymer lamellae.[16,17]

The quantitative determination of the specific interfacial area between polymer and filler is difficult. When the filler is dispersed in a polymeric matrix, traditional methods based on the adsorption of small molecules, i.e., the BET approach, are inapplicable. Image analysis of TEM micrographs can in principle be an option, but it is extremely time-consuming and it suffers from a number of limitations, such as dependence on sample preparation, on projection effects, and on image defocus. Accurate structure−property correlations can only be achieved by developing characterization techniques that allow one to investigate and quantify the interfacial area between the matrix and the filler. The purpose of this paper is that of proposing a SAXS method for the determination of such specific surface area. Such an approach of SAXS data treatment is based on the Porod equation. Although not a new technique (the first publications regarding this equation were published in

Received: April 17, 2012
Published: May 30, 2012

   dx.doi.org/10.1021/jp303685q | J. Phys. Chem. B 2012, 116, 7596−7602

the 1950s),[18] the Porod equation has been used for characterizing catalysts[19,20] or concrete,[21] but it has not been applied, to the knowledge of the authors, to polymer−clay nanocomposites. In this work, complementary techniques such as TEM and X-ray diffraction were applied to confirm the reliability of the results obtained by SAXS. Moreover, in order to test the feasibility of this approach for the development of structure−property relationships, the specific interfacial area obtained by SAXS has been correlated with the physical mechanical properties of rubber−clay nanocomposites.

Three sets of test samples were prepared, one based on natural rubber (NR) and two based on styrene butadiene rubber (SBR), containing different kinds of clay.

2. EXPERIMENTAL SECTION

2.1. Materials. Natural rubber, NR, used for the study was supplied by the Rubber Research Institute of India, Kottayam, Kerala. The average molecular weight of NR obtained by gel permeation chromatography coupled with light scattering is $\bar{M}_n$ = 2.68 × 10^5 g/mol and $\bar{M}_w$ = 8.38 × 10^5 g/mol. Styrene butadiene rubber, 23SBR (1502), was supplied by Premier Rubber Works, Angamaly, Kerala. Organically modified clay (cloisite 10A, cloisite 15A, and cloisite 20A) was obtained from Southern Chemicals, USA. The specifications of the nanoclay used in this study are presented in Table 1. All other ingredients used were of commercial grade and were kindly supplied by LANXESS, Germany.

Table 1. Specifications of Clay[a]

Name of clay	Structure of surfactant	Cation exchange capacity	d_{100} (Å)
Cloisite 10A	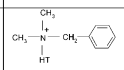	125 meq/100g clay	19.4
Cloisite 15A		125 meq/100g clay	31.5
Cloisite 20A		95 meq/100g clay	24.9

[a]HT = ∼65% C18; ∼30% C16; ∼5% C14.

2.2. Samples and Sample Preparation. The nanocomposite materials were prepared via the melt mixing technique on a laboratory two-roll mill.[22] Formulation of mixes for NR-based samples is shown in Table 2, whereas SBR samples were formulated according to Table 3. The gum matrix was masticated on the two-roll mill for about 2−3 minutes followed by addition of the ingredients. Cure characteristics were studied using an oscillating disc rheometer (Monsanto R-100) at a temperature of 150 °C, thus allowing the optimal cure time to be determined for each sample. The compounds were cured at their respective optimal cure times using a hydraulic press under a pressure of about 120 bar at 150 °C. For the SBR samples, the clay was mixed with SBR by dissolving it in toluene (1 g/50 mL).

Table 2. Formulation of the NR-Based Samples

ingredients	NR (phr)	NR10-2 (phr)	NR10-5 (phr)	NR10-10 (phr)
NR	100	100	100	100
zinc oxide	5	5	5	5
stearic acid	1.5	1.5	1.5	1.5
TMQ[a]	1	1	1	1
CBS[b]	0.6	0.6	0.6	0.6
sulfur	2.5	2.5	2.5	2.5
cloisite 15A	0	2	5	10

[a]2,2,4-Trimethyl-1,2-dihydroquinoline, polymerized. [b]*N*-Cyclohexyl-2-benzothiazyl-sulphenamide.

2.3. Small Angle X-ray Scattering. The SAXS patterns of the samples were recorded by a MBraun system, using Cu Kα radiation from a Philips PW 1830 X-ray generator. The data were collected by a position sensitive detector and were successively corrected for blank scattering, desmeared, and Lorentz-corrected.

2.4. Determination of Interfacial Area by SAXS. Nanocomposites can be modeled as clay particles immersed in a polymer matrix. In this case, the parameter that determines the scattered amplitude, and therefore the scattered intensity, is the difference in electron density $\Delta\rho$ between the "solute", clay in the present case, and the "solvent", i.e., the polymer matrix.

The integral intensity scattered at small angles, also called invariant, Q, is directly related to the mean square fluctuation of electron density, irrespective of the special features of the structure. With a linear collimation geometry, such as the one used in the apparatus employed in this work, $Q = \int_0^\infty 2\pi s I(s)\, ds = (\Delta\rho)^2 V$, where V is the scattering volume, $s = (2 \sin\theta)/\lambda$, θ is the scattering angle, and λ is the wavelength.[19] Alterations or deformations of the structure of part of the system would alter the shape of the diffraction pattern, but the invariant would not change.

In the tail region of the SAXS pattern, the intensity $I(s)$ can be approximated by the so-called Porod law,[18,23] $\lim_{s\to\infty}(I(s)s^3) = (\Delta\rho)^2 S/16\pi^2$, where S is the surface area of the particle. This relationship holds very well, whatever dimension, shape, and porosity of the particles, and it is still valid in concentrated systems because the interferences between particles have little effect on the tail of the SAXS curve. The advantage of this data analysis approach is that it does not require any assumption: the Porod law is verified when the product $I(s) \times s^3$ tends to a constant asymptotic value at large s.[19] This allows the application of this method of SAXS data treatment without any prior assumption on the state of clay dispersion. The practical application of this law for evaluating S requires the measurements of absolute intensity, but introducing the invariant this problem can be avoided and the specific surface can be determined from the diffraction pattern alone, without any additional data:

$$\frac{S}{V} = 16\pi^2 \frac{\lim_{s\to\infty} I(s)s^3}{Q} \quad (1)$$

2.5. Determination of the Average Tactoid Size by the Guinier Equation. The Guinier equation was applied to assess the radius of gyration R of clay particles:[24]

$$I(q) = (\Delta\rho)^2 V^2 \exp\left(-\frac{q^2R^2}{3}\right) \quad (2)$$

where V is the scattering volume. R is the root-mean square of the distances of all electrons from their center of gravity and is related to the physical dimensions of the particles by geometrical relationships. The Guinier formula holds surprisingly well for a wide variety of cases, failing only for very anisometric particles.

dx.doi.org/10.1021/jp303685q | J. Phys. Chem. B 2012, 116, 7596−7602

Table 3. Formulation of the SBR-Based Samples

ingredients	SBR (phr)	SBR10-1 (phr)	SBR10-3 (phr)	SBR10-5 (phr)	SBR15-1 (phr)	SBR15-5 (phr)	SBR15-7 (phr)	SBR20-1 (phr)	SBR20-3 (phr)	SBR20-5 (phr)	SBR20-7 (phr)
23SBR (1502)	100	100	100	100	100	100	100	100	100	100	100
zinc oxide	5	5	5	5	5	5	5	5	5	5	5
stearic acid	2	2	2	2	2	2	2	2	2	2	2
TDQ[a]	1	1	1	1	1	1	1	1	1	1	1
sulfur	2.2	2.2	2.2	2.2	2.2	2.2	2.2	2.2	2.2	2.2	2.2
MBT[b]	1	1	1	1	1	1	1	1	1	1	1
cloisite 10A	0	1	3	5	0	0	0	0	0	0	0
cloisite 15A	0	0	0	0	1	5	7	0	0	0	
cloisite 20A	0	0	0	0	0	0	0	1	3	5	7

[a]2,2,4-Trimethyl-1,2-dihydroquinoline, polymerized. [b]2-Mercaptobenzothiozole.

2.6. Transmission Electron Microscopy. The dispersion of clay was analyzed by transmission electron microscopy (TEM) with a C M 12 PHILIPS HRTEM. Samples for TEM were prepared using an ultramicrotome (Leica, Ultracut UCT), obtaining sections of about 100 nm thickness.

2.7. Measurement of Tensile Properties. Tensile tests were performed according to the ASTM D-412 norm on an Instron 4411 Universal Testing Machine at a cross-head speed of 500 mm/min. Five samples were tested, and the average of the values was taken. The values of tensile strength and modulus were determined.

3. RESULTS AND DISCUSSION

SAXS patterns were acquired for the composites, and the Is^3 vs s^3 plots were computed, for the application of the Porod equation. The specific surface areas obtained by application of eq 1 are summarized in Table 4.

Table 4. Surface Area of Clay in the Considered Samples

sample	interfacial area (m^2/g)	Guinier radius of gyration (nm)
NR10-2	660	10.0
NR10-5	636	9.7
NR10-10	584	10.0
SBR10-1	1308	6
SBR10-3	1114	8.4
SBR10-5	912	9.1
SBR15-1	964	8.8
SBR15-5	1470	6.7
SBR15-7	458	9.7
SBR20-1	1360	5.0
SBR20-3	1134	8.7
SBR20-5	1298	4.6
SBR20-7	1256	4.6
cloisite 10A	654	10.2
cloisite 15A	266	11.0
cloisite 20A	548	13.2

The values of the interfacial area measured for the pristine clays, especially those of cloisite 10A and cloisite 20A, compare well with previously reported values.

Helmy and co-workers[25] quantified the surface area of pure montmorillonite clay by BET, i.e., following the adsorption by clay of molecules of different sizes, obtaining a value of 657.7 m^2/g. The calculated value for the specific surface area of completely exfoliated clay was reported to be 760 m^2/g.[26,27] The specific surface areas measured by BET of the modified clays used in this work are reported in the literature to be in the range 760−780 m^2/g.[28,29]

The data obtained in the present work are somewhat smaller than these values, and indeed smaller in the case of cloisite 15A, showing that the different approaches assess two different aspects of the morphology of the filler.[21] On one hand, BET-like methods exploit the ability of small molecules to penetrate inside the interlayer space of tactoids. On the other hand, SAXS is dependent on the difference in electron density between the tactoids and the matrix. In this case, the relevant difference in electron density is between the tactoid and its surroundings.

The interfacial area values for the composites are less consistent with those reported in the literature for pristine clay. In many instances, much higher values than the calculated surface area were detected. This is again due to the peculiarity of SAXS measurements, which are dependent on the difference in electron density between the tactoid and its surroundings. In the case of composites, the system is more complex than that of pure clay, since the main scattering bodies are clay tactoids, but there may also be contributions from the interfaces of the organocompatibilizer and of the rubber confined within clay tactoids. In other words, the SAXS measurement of the interfacial area comprises all the interfaces in the material: matrix−filler, filler−organocompatibilizer, matrix−organocompatibilizer, etc., so it is reasonable that in some cases the absolute values are higher than expected.

Rather than the absolute value of the interfacial area, it is more interesting to observe the trend of such a feature in the different studied composites.

Applying the Guinier equation (eq 2) on the SAXS patterns, the radii of gyration of the clay dispersed particles were obtained (Table 4). Figure 1 shows the trend of the interfacial

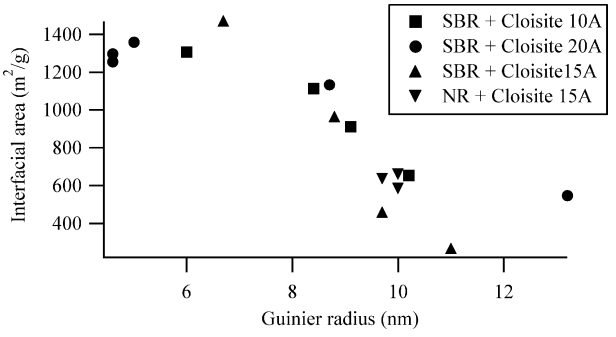

Figure 1. Trend of the matrix/clay interfacial area as a function of the radius of gyration of clay particles.

dx.doi.org/10.1021/jp303685q | J. Phys. Chem. B 2012, 116, 7596−7602

area as a function of the radius of gyration for all the considered samples.

A clear decrease of interfacial area with the increasing size of clay particles was observed, confirming the validity of the approach. When tactoids were smaller than about 7 nm, the interfacial area reached a plateau located at about 1200 m^2/g. Previous observations focused on the relationship between morphology and properties showed that, below a certain tactoid size, further reduction of the number of clay layers in the tactoids did not bring about further significant improvements in the mechanical performance.[30−34]

Pristine clays are characterized by large tactoids, quite tightly stacked, so it is reasonable to find that their interfacial areas are among the smallest.

Figure 2 shows that basically no correlation exists between the interfacial area and *d*-spacing of the clay layers.

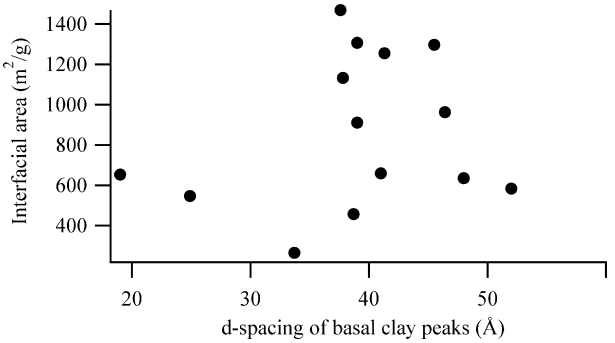

Figure 2. Trend of the matrix/clay interfacial area as a function of the *d*-spacing of the basal clay peaks.

This absence of correlation is mainly due to the fact that the information carried by basal clay peaks is due to only those clay layers that still retain a significantly ordered stacking, and does not take into account single clay layers or disorderly stacked tactoids.[35−37]

As can be noted in Figure 2, composites which share a *d*-spacing of, for example, 40 Å, display a range of interfacial areas going from 400 to about 1400 m^2/g. Obviously, in the case of the samples with a larger interfacial area, the amount of clay layers still stacked in tactoids is much more residual, with respect to those displaying an interfacial area not much different from that of the pristine clay.

For example, it is interesting to compare two of the considered samples, i.e., SBR20-7 and NR15-5. These samples have *d*-spacings of the clay basal peaks of 41.3 and 45 Å, respectively. On the other hand, the radius of gyration of the filler, evaluated by the Guinier equation on the SAXS patterns, in such samples are respectively 3.5 and 10 nm. This is reflected by the TEM micrographs of Figure 3, which show that the composites differ just by the size of tactoids.

SBR20-7 displays thin tactoids and a number of single clay layers. The very good dispersion of clay in this material was corroborated by SAXS, which yielded a featureless trace (Figure 4). On the contrary, NR15-5 shows a more inhomogeneous size distribution, with quite large aggregates in addition to rather small tactoids. This difference in morphology is adequately reflected by the measurement of the interfacial area: SBR20-7 has an interfacial area more than double that of NR15-5. The measurement of interfacial area by SAXS can be especially useful in cases such as those of these samples. In neither case exfoliation was achieved, but in sample SBR20-7 a more extensive dispersion of clay in the matrix was attained with

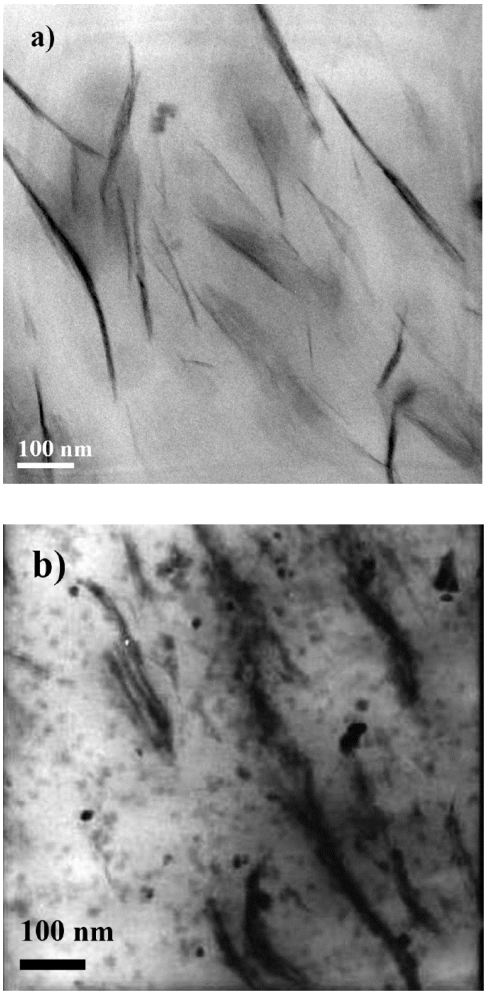

Figure 3. TEM micrographs of samples (a) SBR20-7 and (b) NR15-5.

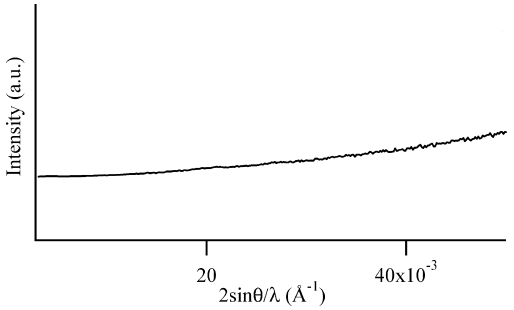

Figure 4. SAXS trace of sample SBR20-7.

respect to sample NR15-5. This can be readily assessed comparing the interfacial areas of the composites.

Very similar considerations can be made comparing other samples among those considered in this study. Almost none of the prepared composites displayed intercalation. In most cases, the morphology was characterized by a coexistence of delaminated layers and of tactoids with a similar interlayer spacing than that of pristine clay. This is consistent with previous speculations that the interaction between polymer and filler does not proceed through a preliminary intercalation step but rather through a progressive peeling of the layers.[31,38] This brings about a decrease in tactoid size, rather than an expansion

dx.doi.org/10.1021/jp303685q | J. Phys. Chem. B 2012, 116, 7596−7602

of the interlayer state. Pristine montmorillonite aggregates are broken down into much smaller stacks.[39]

In order to assess the usefulness of the measurement of interfacial area for the development of structure−property relationships, the effect of such a feature on mechanical properties was investigated. The interfacial area is known to influence very strongly the physical mechanical properties of composites. Table 5 reports the tensile properties of the composites based on NR and of the SBR-based composites filled with cloisite 10A and 20A.

Table 5. Tensile Properties and Total Interfacial Area of Selected Samples

sample	total interfacial area (m^2/100 g of composite)	modulus (MPa)	tensile strength (MPa)	elongation at break (%)
NR		1.07	16.91	617
NR10-2	1320	1.21	20.29	605
NR10-5	3180	1.70	20.47	587
NR10-10	5840	2.19	20.71	594
SBR		1.15	2.05	309
SBR10-1	1308	1.29	3.3	442
SBR10-3	3723	1.43	4.3	542
SBR10-5	4560	1.67	5.4	698
SBR20-1	1360	1.35	3.1	334
SBR20-3	3402	1.48	3.6	578
SBR20-5	6490	1.55	4.8	513
SBR20-7	8792	1.8	6.75	857

Since in this system the scattering bodies are mainly clay tactoids and layers, an estimate of the total interfacial area in each composite can be obtained by multiplying the specific surface area by the filler percentage (w/w). Obtained data are reported in Table 5. The total interfacial area shows an increasing trend with filler content. It is well-known that a large contact surface coupled with strong interaction of the components leads to significant increases in stiffness.[5,6] Figure 5 confirms that the enlargement of the total interfacial area has the consequence of increasing the modulus.

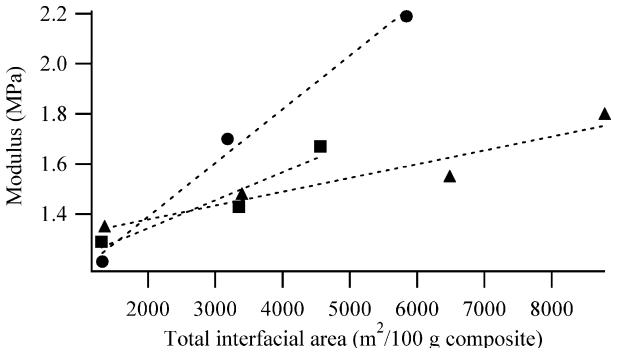

Figure 5. Elastic modulus as a function of interfacial area. Circles indicate samples of the NR series, squares indicate samples of the SBR10 series, and triangles indicate samples of the SBR20. The lines were added just to guide the eye.

In Figure 6, the experimental trend of modulus as a function of volume fraction of filler is shown. The Halpin−Tsai equation[40] was used to fit the experimental points

$$\frac{E_c}{E_m} = \frac{1 + \xi\eta\varphi}{1 - \eta\varphi} \tag{8}$$

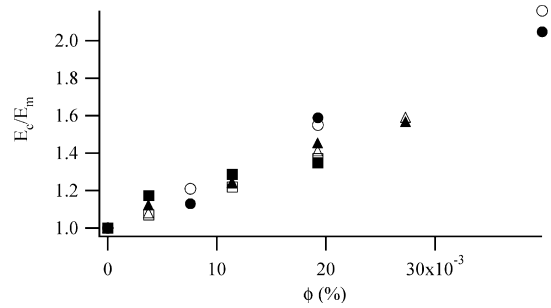

Figure 6. Elastic modulus as a function of the volume fraction of filler φ. Circles indicate samples of the NR series, squares indicate samples of the SBR10 series, and triangles indicate samples of the SBR20. Closed symbols indicate experimental data, and open symbols correspond to the values calculated according to the Halpin−Tsai equation.

where E_c and E_m are the elastic moduli of the composite and the matrix, respectively, φ is the volume fraction of the filler, ξ is the aspect ratio multiplied by 2, and η is given by

$$\eta = \frac{(E_f/E_m) - 1}{(E_f/E_m) + \xi} \tag{9}$$

where E_f is the elastic modulus of the filler, i.e., 178 GPa for montmorillonite.[41] By fitting the experimental data by the Halpin−Tsai equation, an aspect ratio between 10 and 15 was obtained for the three considered sample series. This value is comparable but lower than that found by Fornes and Paul[42] for almost exfoliated organoclay, i.e., 57. The aspect ratios obtained in our samples therefore agree with SAXS data: a good dispersion of clay in the matrix was achieved by a decrease in tactoid size, although no exfoliation was observed.

Usually, the increase in stiffness is interpreted as a proof that reinforcement by the filler occurred. However, indication of efficient reinforcement can be found only if stiffness and strength increase simultaneously, as noted by Pukánsky.[5,7,43,44] These authors proposed a very reliable approach to a quantitative estimation of reinforcement by exploiting ultimate properties.[44] According to this model, the dependence of tensile strength on the volume fraction of filler is given by the following:[44]

$$\sigma_T = \sigma_{T_0}\lambda^n \frac{1 - \varphi}{1 + 2.5\varphi} \exp(B\varphi) \tag{10}$$

where the true tensile strength ($\sigma_T = \sigma\lambda$, $\lambda = L/L_0$, relative elongation) accounts for the change in specimen cross section and λ^n for strain hardening. n characterizes the strain hardening tendency of the polymer. It was calculated from the log σ_T vs log λ curve of the matrix polymer,[44] and it was found to be equal to 0.95. σ_{T_0} is the true tensile strength of the pure matrix. B is a parameter dependent on the size of the interface and on the strength of the interphase, which quantifies the reinforcement due to the filler in the composite. The larger B is, the greater is the reinforcement. The logarithm of $\sigma_{T_{Rel}}$, the relative true tensile strength, $\sigma_{T_{Rel}} = (\sigma_T/\sigma_{T_0}\lambda^n)[(1 + 2.5\varphi)/(1 - \varphi)]$, was plotted as a function of φ (Figure 7). Straight lines were obtained, which by linear regression yielded $B = 9$ for the NR−cloisite 15A series and $B = 84$ and 67 for the samples based on SBR and filled with cloisite 10A and 20A, respectively.

As a term of comparison, the highest published B value was obtained by adding a filler with a surface area of 200 m^2/g to a low density polyethylene (LDPE) matrix, which yielded a B

dx.doi.org/10.1021/jp303685q | J. Phys. Chem. B 2012, 116, 7596−7602

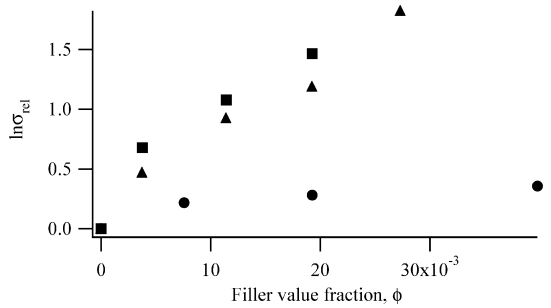

Figure 7. Linearized function of the true tensile strength of the samples as a function of filler content. Circles represent the samples of the NR series, squares represent samples of the SBR10 series, and triangles represent samples of the SBR20 series.

value of 11.36.[44] It should be remarked that *B* is also dependent on the nature of the matrix, and especially on its true tensile strength, but LDPE shares a comparable typical tensile strength (15.2−78.6 MPa)[45] with respect to natural rubber (18−21 MPa),[45] although rubber usually has a larger elongation at break.

Completely exfoliated clay is expected to yield a value of the parameter *B* of around[5] 195 in PP, and this number should be larger in rubber. Since *B* depends on the surface area of the filler, the value obtained for our samples can be interpreted as a confirmation of the very large specific surface area measured by SAXS in the SBR-based samples, although the data do not allow us to conclude complete exfoliation. However, the focus of this paper was not that of achieving a particular degree of dispersion of clay in the polymer matrix but that of obtaining a reliable method for estimating the extent of matrix−filler interfacial area. Under this point of view, the results of the application of the Porod equation to SAXS patterns were in agreement with the trend of mechanical properties dependent on the matrix−filler interfacial area, thus confirming the feasibility of this approach of SAXS data treatment.

4. CONCLUSION

A very easy SAXS method for measuring the specific surface area of nanofillers embedded in a polymer matrix was proposed. Fitting of the SAXS patterns according to the Porod equation allowed this parameter to be estimated, which would be very hard to obtain by alternative methods. In order to check the reliability of such an approach, we investigated several natural rubber and stryrene butadiene rubber samples containing different kinds and amounts of montmorillonite clay, detecting wide differences in the dispersion of clay as a function of their formulation. The data on interfacial area obtained by the Porod equation were crossed with WAXD, SAXS, TEM and tensile testing data, in order to obtain a thorough picture of the extent of clay dispersion in the samples, and thus on interfacial area. Porod results were in good agreement with all these complementary techniques, confirming then that this approach in SAXS data treatment allows a parameter to be estimated, the specific interfacial area between matrix and filler, which needs extensive efforts if one wants to characterize it by other methods.

Another interesting result that emerged from this work is that no significant intercalation was detected in any of the samples but rather reduction in tactoid size. This seems to support the hypothesis that exfoliation does not occur through an intercalation-mediated mechanism but rather through a progressive peeling of the outer layers of the tactoids.

AUTHOR INFORMATION

Corresponding Author

*Phone: +39-049-8275215. Fax: +39-049-8275161. E-mail: valerio.causin@unipd.it.

Notes

The authors declare no competing financial interest.

REFERENCES

(1) Usuki, A.; Kawasumi, M.; Kojima, Y.; Okada, A.; Kurauchi, T.; Kamigaito, O. *J. Mater. Res.* **1993**, *8*, 1174−1178.
(2) de Paiva, L. B.; Morales, A. R.; Valenzuela Diaz, F. R. *Appl. Clay Sci.* **2008**, *42*, 8−24.
(3) Ray, S. S.; Okamoto, M. *Prog. Polym. Sci.* **2003**, *28*, 1539−1641.
(4) Tjong, S. C. *Mater. Sci. Eng., R* **2006**, *53*, 73−197.
(5) Százdi, L.; Pukánszky, J. B.; Vancso, G. J.; Pukánszky, B. *Polymer* **2006**, *47*, 4638−4648.
(6) Reichert, P.; Nitz, H.; Klinke, S.; Brandsch, R.; Thomann, R.; Mülhaupt, R. *Macromol. Mater. Eng.* **2000**, *275*, 8−17.
(7) Móczó, J.; Pukánszky, B. *J. Ind. Eng. Chem.* **2008**, *14*, 535−563.
(8) Adhikari, R.; Michler, G. H. *Polym. Rev.* **2009**, *49*, 141−180.
(9) Causin, V.; Marega, C.; Marigo, A.; Ferrara, G. *Polymer* **2005**, *46*, 9533−9537.
(10) Vaia, R. A.; Liu, W. *J. Polym. Sci., Part B: Polym. Phys.* **2002**, *40*, 1590−1600.
(11) Vaia, R. A.; Liu, W.; Koerner, H. *J. Polym. Sci., Part B: Polym. Phys.* **2003**, *41*, 3214−3236.
(12) Gelfer, M.; Burger, C.; Fadeev, A.; Sics, I.; Chu, B.; Hsiao, B. S.; Heintz, A.; Kojo, K.; Hsu, S.; Si, M.; Rafailovich, M. *Langmuir* **2004**, *20*, 3746−3758.
(13) Ruland, W.; Smarsly, B. *J. Appl. Crystallogr.* **2004**, *37*, 575−584.
(14) Kaneko, M. L. Q. A.; Torriani, I. L.; Yoshida, I. V. P. *J. Braz. Chem. Soc.* **2007**, *18*, 765−773.
(15) Dykes, L. M. C.; Torkelson, J. M.; Burghardt, W. R.; Krishnamoorti, R. *Polymer* **2010**, *51*, 4916−4927.
(16) Lincoln, D. M.; Vaia, R. A.; Wang, Z. G.; Hsiao, B. S.; Krishnamoorti, R. *Polymer* **2001**, *42*, 9975−9985.
(17) Lincoln, D. M.; Vaia, R. A.; Krishnamoorti, R. *Macromolecules* **2004**, *37*, 4554−4561.
(18) Porod, G. *Kolloid Z.* **1951**, *124*, 83−114.
(19) Gallezot, P. X-ray techniques in catalysis. In *Catalysis. Science and Technology*; Anderson, J. R., Boudart, M., Eds.; Springer: Berlin, 1984; Vol. *5*.
(20) Marigo, A.; Marega, C.; Zannetti, R.; Morini, G.; Ferrara, G. *Eur. Polym. J.* **2000**, *36*, 1921−1926.
(21) Tritthart, J.; Haussler, F. Small Angle Neutron Scattering as well as pore solution investigations of cement. In *Frost resistance of concrete*; Setzer, M. J., Auberg, R., Keck, H. J., Eds.; RILEM Publications: Cachan, France, 2002.
(22) Sadhu, S.; Bhowmick, A. K. *J. Appl. Polym. Sci.* **2004**, *92*, 698−709.
(23) Debye, P.; Anderson, H. R. J.; Brumberger, H. *J. Appl. Phys.* **1957**, *28*, 679−683.
(24) Guinier, A. *Ann. Phys.* **1939**, *12*, 161−236.
(25) Helmy, A. K.; Ferreiro, E. A.; de Bussetti, S. G. *J. Colloid Interface Sci.* **1999**, *210*, 167−171.
(26) LeBaron, P. C.; Wang, Z.; Pinnavaia, T. J. *Appl. Clay Sci.* **1999**, *15*, 11−29.
(27) Theng, B. K. G. *Formation and properties of clay-polymer complexes*; Elsevier: Amsterdam, The Netherlands, 1979.
(28) Tran, T. A.; Said, S.; Grohens, Y. *Macromolecules* **2005**, *38*, 3867−3871.
(29) Okamoto, M. In Polymer/layered silicate nanocomposites: a review. In *Handbook of biodegradable polymeric materials and their applications*; Mallapragada, S., Narasimban, B., Eds.; American Scientific Publisher: Valencia, CA, 2005.
(30) Causin, V.; Marega, C.; Marigo, A.; Ferrara, G.; Ferraro, A.; Selleri, R. *J. Nanosci. Nanotechnol.* **2008**, *8*, 1823−1834.

(31) Marega, C.; Causin, V.; Marigo, A.; Ferrara, G. *J. Appl. Polym. Sci.* **2009**, *113*, 3920−3928.
(32) Mehta, S.; Mirabella, F. M.; Rufener, K.; Bafna, A. *J. Appl. Polym. Sci.* **2004**, *92*, 928−936.
(33) Fasulo, P. D.; Rodgers, W. R.; Ottaviani, R. A.; Hunter, D. L. *Polym. Eng. Sci.* **2004**, *44*, 1036−1045.
(34) Vermogen, A.; Masenelli-Varlot, K.; Vigier, G.; Sixou, B.; Thollet, G.; Duchet-Rumeau, J. *J. Nanosci. Nanotechnol.* **2007**, *7*, 3160−3171.
(35) Ma, J.; Yu, Z. Z.; Kuan, H. C.; Dasari, A.; Mai, Y. W. *Macromol. Rapid Commun.* **2005**, *26*, 830−833.
(36) Jin, Y. H.; Park, H. J.; Im, S. S.; Kwak, S. Y.; Kwak, S. *Macromol. Rapid Commun.* **2002**, *23*, 135−140.
(37) Hoffmann, B.; Dietrich, C.; Thomann, R.; Friedrich, C.; Mülhaupt, R. *Macromol. Rapid Commun.* **2000**, *21*, 57−61.
(38) Galimberti, M.; Lostritto, A.; Spatola, A.; Guerra, G. *Chem. Mater.* **2007**, *19*, 2495−2499.
(39) Min, K. D.; Kim, M. Y.; Choi, K. Y.; Lee, J. H.; Lee, S. G. *Polym. Bull.* **2006**, *57*, 101−108.
(40) Halpin, J. C.; Kardos, J. L. *Polym. Eng. Sci.* **1976**, *16*, 344−352.
(41) Chen, B.; Evans, J. R. G. *Scr. Mater.* **2006**, *54*, 1581−1585.
(42) Fornes, T. D.; Paul, D. R. *Polymer* **2003**, *44*, 4993−5013.
(43) Százdi, L.; Pozsgay, A.; Pukánszky, B. *Eur. Polym. J.* **2007**, *43*, 345−359.
(44) Pukánszky, B. *Composites* **1990**, *21*, 255−262.
(45) Brandrup, J.; Immergut, E. H.; Grulke, E. A. *Polymer Handbook*; Wiley: New York, 1999.